Numerical modelling of groundwater flow around contiguous pile retaining walls

Modélisation numérique des écoulements des eaux souterraines autour d'écrans de soutènement de pieux contigusë

Wiggan C. A., Richards D.J., Powrie W.
University of Southampton, Southampton SO17 1BJ, United Kingdom

ABSTRACT: Pore water pressure constitutes a significant proportion of the lateral load acting on a retaining wall. Consequently, guidelines often mandate that the worst case hydraulic conditions are applied in the design of retaining walls. This invariably dictates that retaining walls are treated as impermeable unless special consideration is given to the maintenance of drainage systems or to the prevention of infiltration. Contiguous pile retaining walls are, however, by their nature permeable unless considerable effort is expended to prevent seepage through gaps. If allowed, this seepage can result in reduced active side pore water pressures. Numerical simulations were conducted to determine the impact on pore water pressures of varying the pile gap (x) to diameter (d) ratio, x/d, in a contiguous pile retaining wall. A relationship between x/d and the effective bulk wall permeability, k_p was derived, and applied to two-dimensional simulations representing a contiguous pile wall. The results show that pore pressures behind the retaining wall reduced significantly with increased x/d.

RÉSUMÉ: La pression de l'eau interstitielle constitue une part importante des charges latérales agissant sur les parois d'un mur de soutènement. Par conséquent, les règles de l'art imposent que les pires conditions hydrauliques soient considérées dans la conception d'un mur de soutènement. Cela impose invariablement que les murs de soutènement soient considérés comme imperméables à moins que des considérations particulières soient données à l'entretien des systèmes de drainage ou à la prévention des infiltrations. Les murs de soutènement constitués de pieuxcontigus, sont cependant perméables (de par leur structure), à moins que des efforts considérables soient déployés pour empêcher les infiltrations à travers les intervalles. Ces infiltrations peuvent entrainer une réduction des pressions interstitielles effectives. Des simulations numériques ont été réalisées afin de déterminer l'impact des variations de l'espace entre palplanches (x), de diamètre (d), de ratio, x /d, sur les pressions interstitielles d'un mur de soutènement constitué de pieux contigus. Une relation entre le ratio x/d et la réelle perméabilité du mur, k_p a été déduite et appliquée à un modèle à deux dimensions représentant un mur en pieuxcontigus. Les résultats montrent que les pressions interstitielles derrière le mur de soutènement diminuent significativement lorsque le ratio x/d augmente.

KEYWORDS: Pore water pressure, numerical modelling, retaining wall, seepage forces, surface settlement

1 INTRODUCTION

Guidelines generally require that the most onerous tenable pore water pressure distribution is adopted for the design of subsurface retaining structures. For example, Eurocode 7 recommends that, unless reliable drainage can be provided or infiltration prevented, retaining walls should be designed with the water table at the ground surface (BSI, 2004). This can however cause over-conservative and unnecessarily expensive engineering solutions which go against the ethos of sustainable development. It would be advantageous if, based on the bulk permeability of the structure, the hydraulic loads on retaining walls could be treated as reduced.

There is however limited research into how the geometry influences hydraulic loads on retaining walls although, according to CIRIA 580, 'economic advantages' might be derived if through-wall seepage is allowed (Gaba et al. 2003). This is due mainly to the reduction in pore pressures because of through-wall seepage. Research into ways of facilitating through-wall seepage and quantifying its effect is necessary.

1.1 *Research in hydraulic loads around retaining structures*

Previous research has not generally sought to distinguish between the long-term pore water pressure distributions around different types of retaining walls. For example, Potts and Burland (1983) and Hubbard et al. (1984) showed that the long-term pore pressures behind a secant pile retaining wall recovered to near their pre-construction values as might be expected of an impermeable wall in fine soils. Powrie et al. (1999) and Carder et al. (1999) observed a reduction in pore pressures following construction of a contiguous pile retaining wall at Woodford. The pore pressures at Woodford however, did not return to their pre-construction values in the long-term. This reduction was attributed at the time to under-drainage to the more permeable chalk layer and therefore no consideration was given to the possible contribution of through-wall seepage. However Clark (2006) and Richards et al. (2007) have shown that there was a reduction in long-term pore pressures measured at a contiguous pile retaining wall in over-consolidated clay at Ashford. The pore pressures have not returned to their pre-construction values. Although there is underdrainage to the more permeable Weald Clay at Ashford, there is evidence that the long-term reduction in pore pressure can be attributed to through-wall seepage.

In contrast to retaining walls, there has been significant research into methods of reducing pore water pressures acting on shallow tunnels and on tunnels acting as drains. Despite an earlier assumption by Atkinson and Mair (1983) that groundwater loadings do not change significantly in the presence of varying hydraulic conditions, it has been shown by numerical analyses that segmented tunnel linings do in fact allow seepage of groundwater which contributes to reduced pore water pressures around tunnels in fine grained soils. Pore pressures at segmented lined tunnels approach atmospheric values and increase with distance away from the tunnel (Shin et al. (2002), Lee and Nam (2006), Bobet and Nam (2007) and Arjnoi et al. (2009)).

The corresponding reductions in axial forces and stresses on segmented tunnel linings in comparison with fully waterproofed linings are significant, although inconsistent. For example Arjnoi et al (2009) observed a 20% reduction, Lee and Nam (2001) 25%, Potts et al. (2002) up to 30% and Lee and Nam (2006) up to a 70% reduction.

1.1.1 *Surface settlement*

Notwithstanding the potential advantages of allowing through-structure seepage, some detrimental effects have been noted in the analyses of shallow tunnels which might be relevant to through-wall seepage. Significant settlements have been observed associated with segmented lined tunnels acting as drains in fine grained soils. For example, Yoo (2005) noted that settlement was proportional to the amount of drawdown in the groundwater levels around the tunnel. Consolidation settlement, ρ due to the drawdown of groundwater level may be estimated in a similar manner by considering the one dimensional stiffness modulus, E'_0 of the soil as shown in equations 1 and 2 (Roberts et al. 2007).

$$E'_0 = 400\sigma'_v \quad (1)$$

$$\rho = \frac{D\gamma_w S_{av}}{E_{0av}} \quad (2)$$

where σ'_v, D, γ_w and S_{av} are the vertical effective stress, thickness of the soil layer, unit weight of water and average drawdown respectively.

In this paper, pore water pressure variations around contiguous pile retaining walls are investigated numerically. An expression for the resulting effective bulk wall permeability k_p, is derived. This is then applied to two dimensional analyses of contiguous and secant pile retaining walls to highlight the advantages of a semi-permeable structure.

2 NUMERICAL ANALYSES

Numerical simulations were conducted using the finite difference geotechnical application FLAC2D (ITASCA, 2012). The investigations were undertaken in two phases. Horizontal flow was simulated in phase 1 to determine how pore pressures and steady state flow vary with x/d in order to derive an expression for k_p/k_s. This relationship was then applied to a vertical plane flow in phase 2 and the pore pressures calculated.

Preliminary analysis, not included in this report, were carried out to establish i) suitable boundary locations, ii) the size of the numerical grid and iii) the limiting value of x/d. Grid boundaries were selected such that x/d did not influence the far-field conditions. It was determined that increasing x/d above 2 did not significantly impact the results.

2.1 *Model soil and wall properties*

An elastic constitutive soil model was used in all analyses. Elastic properties of bulk and shear moduli were used instead of Young's modulus and Poisson's ratios. The soil and model pile section and the model wall in phases 1 and 2 respectively were represented by grid elements attached directly to the soil grid without the use of interface elements so as to allow cross-boundary flow. Uncoupled groundwater flow analyses which ignored the impact of mechanically induced pore pressures were performed.

2.2 *Derivation of bulk wall permeability, k_p*

The simulations started with a 'wished into place' model pile section and the water level at the surface. Pore pressures at the discharge surface shown in figure 1 were lowered incrementally corresponding to pressure drops U_i for each step. Steady state discharge and pore pressures were measured and fluid flow-paths tracked for different pile gap to diameter ratios x/d.

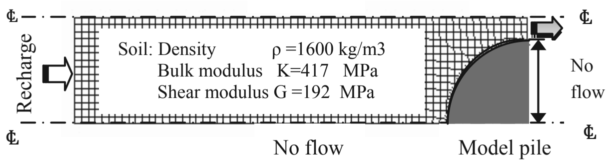

Figure 1. Plan of typical numerical grid showing boundary conditions for phase 1 analyses.

2.2.1 *Results and discussion*

Darcy's equation for steady state flow (Eq. 3) was applied using the parameters Δl, h_1, and h_2 indicated in figure 2 and the values compared with the numerically derived flow rates (Q_i) in figure 3 at pressure differences, U_i.

$$Q = A_p k_p \frac{h_1 - h_2}{\Delta l} \quad (3)$$

where $(h_1\text{-}h_2)/\Delta l$ is the hydraulic gradient between the distance of influence and the discharge surface (see Figure 2). (The distance of influence was selected as the point beyond which the hydraulic gradient was uniform).

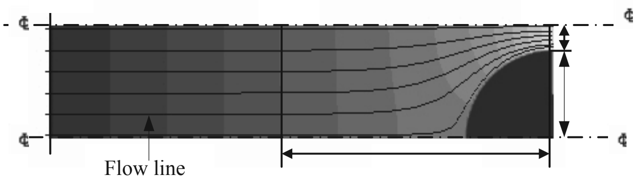

Figure 2. Calculating bulk wall permeability, k_p and flow-paths.

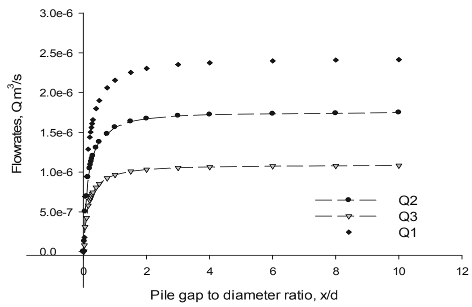

Figure 3. Steady state flow-rates, Q_i at various pressure drops U_i.

The resulting bulk wall permeability was calculated for a soil permeability $k_s=2\times10^{-5}$ m/s and plotted for three values of U_i (see Figure 4). The empirical hyperbolic relationship between the pile gap to diameter ratios x/d and permeability ratios k_p/k_s derived in the phase 1 simulation is given in equation 4.

$$\frac{k_p}{k_s} = \frac{4\frac{x}{d}}{1+4\frac{x}{d}} \quad (4)$$

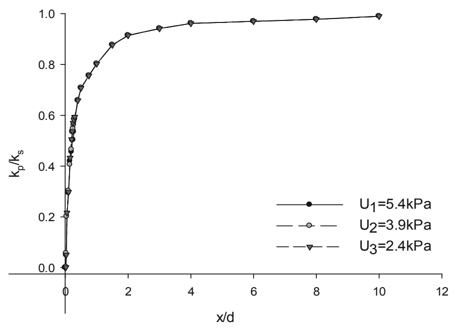

Figure 4. Calculated permeability from FLAC2D simulations.

2.3 *Application of derived expression to 2D analyses*

The aim of phase 2 simulations was to test the application of the permeability expression derived in phase 1.

2.3.1 *Procedure*

A continuous wall was used to represent the contiguous pile retaining wall. The model wall thickness (t) was calculated by equating the second moments of area (I) of the different cross-sections (A) as outlined by Powrie et al (1999) (Eq. 5). This gave a result similar to the stiffness approach adopted by Day and Potts (1993) (see Eq. 6 and 7).

$$I_p = I_m \quad (5)$$

$$tE_{eq} = EA \quad (6)$$

$$E_{eq} = EI \quad (7)$$

where E_{eq} and E are the equivalent model wall stiffness and material Young's modulus respectively.

The simulations commenced as before with a 'wished into place' model wall. Pore pressures were varied corresponding to U_i as before for different pile gap to diameter ratios, x/d.

2.3.2 *Results and discussion*

It was observed that flow patterns for the 'permeable' walls deviated from the classically accepted flow around an impermeable retaining wall especially at higher values of x/d. This seems to suggest that through-wall flow is taking place for x/d>0.0 as shown in figure 5.

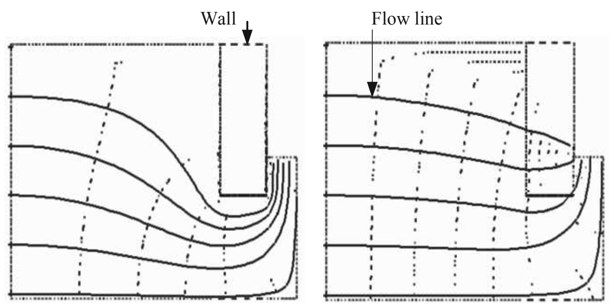

Figure 5. Tracked flow-paths for x/d=0 and x/d=0.1. Note these are not intended to be flownets, hence the flow elements are not "square".

2.3.3 *Pore pressure distribution*

Pore pressures ratios P_i/P_0 are plotted against normalized distance (L/d) from the model wall in figure 6 for various values of x/d.

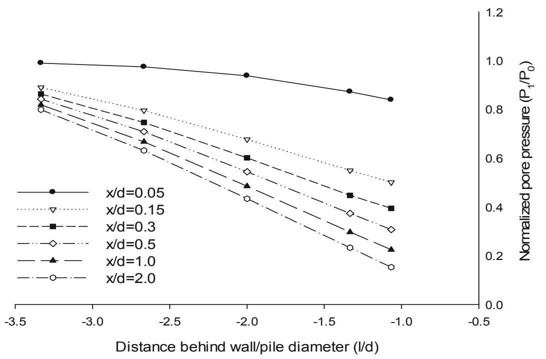

Figure 6. Normalised pore pressures for different x/d against distance (L/d) from the wall.

It was observed that pore pressures at each position behind the wall decreased with x/d as the equivalent permeability increased. Further analyses have shown that the pore pressures and hence hydraulic head reduce towards the wall (Figure 7).

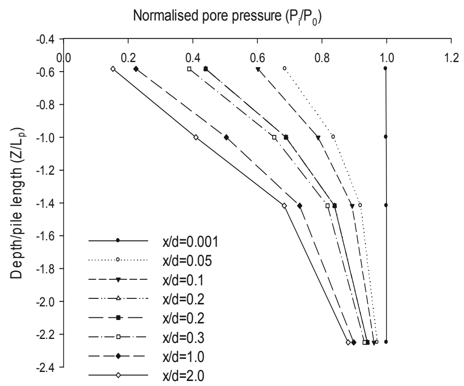

Figure 7. Normalised pore pressure versus normalized depth below soil surface for different values of x/d.

2.3.4 *The effect of seepage on surface settlement*

Surface settlements increased as the bulk permeability of the wall increased (see Figure 8). The calculated settlement values were compared with an estimated solution which uses the one dimensional stiffness modulus (Roberts et al 2007). It was noted that the 1D stiffness modulus method over-predicted surface settlement at higher x/d as shown in Figure 9. This is unsurprising as in this approach all volume change is assumed to manifest as vertical settlement.

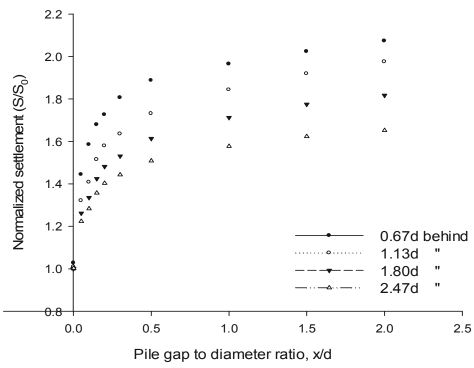

Figure 8. Normalised settlement increases with soil/structure permeability.

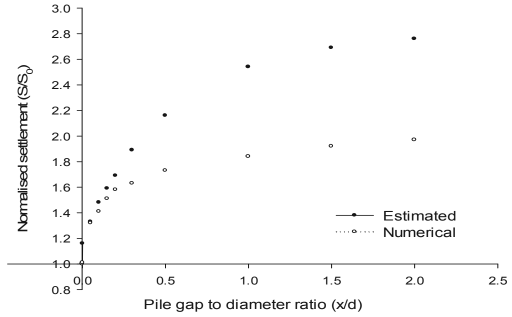

Figure 9. Comparison of analytical and numerical solutions for surface settlement variation with x/d.

2.5 *Secant versus Contiguous Pile Retaining Walls*

Comparisons were made between retaining walls formed of contiguous and secant piles 20m long with 10m excavation depth in homogeneous soil. Figure 10 shows that the pore pressure profiles are slightly less than hydrostatic for the secant and significantly less than hydrostatic for the contiguous pile wall.

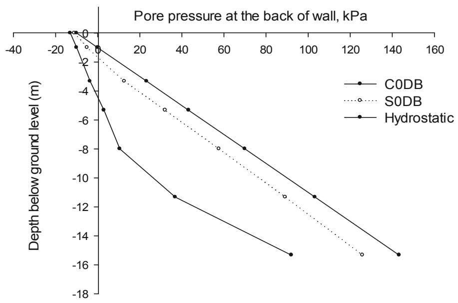

Figure 10. Comparison of pore pressure profiles for secant and contiguous pile walls against hydrostatic pressure.

3 CONCLUSIONS

Limited research has previously been carried out on the influence of retaining wall geometry on the development of hydraulic loads on the active side. Numerical simulations presented in this paper have shown that the pore pressure magnitude behind bored pile retaining walls reduces with increasing pile gap to diameter ratio, x/d. This reduction in lateral loads however is accompanied by an increase surface settlement. However, the potential benefits of allowing through-wall seepage are likely to be greater than the drawbacks.

4 ACKNOWLEDGEMENTS

Funding for this research was provided by the Engineering and Physical Sciences Research Council, (EPSRC) grant number EP/F063482.

5 REFERENCES

Arjnoi, P., Jeong, J.H., Kim, C.Y., & Park, K.H. 2009. Effect of drainage conditions on porewater pressure distributions and lining stresses in drained tunnels. Tunnelling and Underground Space Technology, 24, (4) 376-389.

Atkinson, J.H. & Mair, R.J. 1983. Loads on Leaking and Watertight Tunnel Linings, Sewers and Buried Pipes due to Groundwater. Geotechnique, 33, (3) 341-344

Bobet, A. & Nam, S.W. 2007. Stresses around pressure tunnels with semi-permeable liners. Rock Mechanics and Rock Engineering, 40, (3) 287-315.

BSI 2004, Eurocode 7: Geotechnical design Part 1, General Rules. EN1997-1:2004, British Standard Institution.

Carder, D.R., Watson, G.V.R., Chandler, R.J., & Powrie, W. 1999. Long-term performance of an embedded retaining wall with a stabilizing base slab. Proceedings of the Institution of Civil Engineers-Geotechnical Engineering, 137, (2) 63-74.

Clark, J. 2006. Performance of a propped retaining wall at the Channel Tunnel Rail Link, Ashford. PhD University of Southampton.

Day, R.A. & Potts, D.M. 1993. Modeling Sheet Pile Retaining Walls. Computers and Geotechnics, 15, (3) 125-143

Gaba, A.R., Simpson, B., Beadman, D.R., & Powrie, W. 2003. Embedded retaining walls: guidance for economic design. Proceedings of the Institution of Civil Engineers-Geotechnical Engineering, 156, (1) 13-15.

Hubbard, H.W., Potts, D.M., & Miller, D. 1984. Design of the retaining walls for the M25 cut and cover tunnel at Bell Common. Geotechnique, 34, (4) 495-512

ITASCA. Fast Langrangian Analysis of Continua in 2 Dimensions. User Manual. Itasca Consulting Group[7.0]. 2012. Minneapolis, USA. Ref Type: Computer Program

Kolymbas, D. & Wagner, P. 2007. Groundwater ingress to tunnels - The exact analytical solution. Tunnelling and Underground Space Technology, 22, (1) 23-27.

Lee, I. M. & Nam, S. W. 2001, The study of seepage forces acting on tunnel lining and tunnel face in shallow tunnels. Tunnelling and Underground Space Technology, 16, (1) 31-40.

Lee, I. M. & Nam, S. W. 2006, Seepage Force Considerations in Tunnelling, In International Symposium on Underground Excavation and Tunnelling.

Potts, D. M., Axelsson, K., Grande, L., Schweiger, H., & Long, M. Guidelines for the use of advanced numerical analysis. 2002. Thomas Telford Publishing. Ref Type: Edited Book

Potts, D. M. & Burland, J. B. 1983, Numerical investigation of retaining wall at Bell Common Tunnel.

Powrie, W., Chandler, R.J., Carder, D.R., & Watson, G.V.R. 1999. Back-analysis of an embedded retaining wall with a stabilizing base slab. Proceedings of the Institution of Civil Engineers-Geotechnical Engineering, 137, (2) 75-86.

Richards, D.J., Powrie, W., Roscoe, H., & Clark, J. 2007. Pore water pressure and horizontal stress changes measured during construction of a contiguous bored pile multi-propped retaining wall in Lower Cretaceous clays. Geotechnique, 57, (2) 197-205.

Roberts, T.O.L., Roscoe, H., Powrie, W., & Butcher, D.J.E. 2007. Controlling clay pore pressures for cut-and-cover tunnelling. Proceedings of the Institution of Civil Engineers-Geotechnical Engineering, 160, (4) 227-236.

Shin, J.H. 2010. Analytical and combined numerical methods evaluating pore water pressure on tunnels. Geotechnique, 60, (2) 141-145.

Shin, J.H., Addenbrooke, T.I., & Potts, D.M. 2002. A numerical study of the effect of groundwater movement on long-term tunnel behaviour. Geotechnique, 52, (6) 391-403.

Yoo, C.S. 2005. Interaction between tunnelling and groundwater, Numerical investigation using three dimensional stress pore pressure coupled analysis. *Journal of Geotechnical and Geoenvironmental Engineering, 131,)2= 497ß513.*